

Depletion of Nonlinearity in Magnetohydrodynamic Turbulence: Insights from Analysis and Simulations

J. Gibbon¹, A. Gupta², G. Krstulovic³, R. Pandit⁴, H.

Politano⁵, Y. Ponty³, A. Pouquet^{6,7}, G. Sahoo², and J. Stawarz⁷

¹*Department of Mathematics, Imperial College London, London SW7 2AZ, UK.*

²*Department of Physics, University of Rome ‘Tor Vergata’, 00133 Roma, Italy.*

³*Laboratoire Lagrange, Université Côte d’Azur, Observatoire de la Côte d’Azur, CNRS, Blvd de l’Observatoire, CS 34229, 06304 Nice cedex 4, France*

⁴*Centre for Condensed Matter Theory, Indian Institute of Science, Bangalore, 560 012, India.*

⁵*Laboratoire Dieudonné, Université de Nice, France.*

⁶*National Center for Atmospheric Research,*

P.O. Box 3000, Boulder, CO 80307, USA.

⁷*Laboratory for Atmospheric and Space Physics,*

University of Colorado, Boulder, CO 80303, USA.

We build on recent developments in the study of fluid turbulence [Gibbon *et al.* Nonlinearity 27, 2605 (2014)] to define suitably scaled, order- m moments, D_m^\pm , of $\omega^\pm = \omega \pm \mathbf{j}$, where ω and \mathbf{j} are, respectively, the vorticity and current density in three-dimensional magnetohydrodynamics (MHD). We show by mathematical analysis, for unit magnetic Prandtl number P_M , how these moments can be used to identify three possible regimes for solutions of the MHD equations; these regimes are specified by inequalities for D_m^\pm and D_1^\pm . We then compare our mathematical results with those from our direct numerical simulations (DNSs) and thus demonstrate that 3D MHD turbulence is like its fluid-turbulence counterpart insofar as all solutions, which we have investigated, remain in *only one of these regimes*; this regime has depleted nonlinearity. We examine the implications of our results for the exponents q^\pm that characterize the power-law dependences of the energy spectra $\mathcal{E}^\pm(k)$ on the wave number k , in the inertial range of scales. We also comment on (a) the generalization of our results to the case $P_M \neq 1$ and (b) the relation between D_m^\pm and the order- m moments of gradients of hydrodynamic fields, which are used in characterizing intermittency in turbulent flows.

PACS numbers: 47.27.Ak, 52.30.Cv, 47.27.ek, 02.30.Jr

Intermittency is widespread in nature: the characterization of such intermittency is a central problem in turbulence [1–9], in nonequilibrium statistical mechanics, in the production and storage of wind and solar energy, and the behaviors of market crashes and of several critical phenomena [10, 11]. Such intermittency has been studied extensively in fluid turbulence [1, 3–9] and in magnetohydrodynamic (MHD) turbulence [12–16], often by using order- p structure functions of fields such as the velocity and, in MHD, also the magnetic field. An example is the (longitudinal) velocity \mathbf{v} structure function $S_p(r) \equiv \langle [\delta v(r)]^p \rangle$, where $\delta v(r) \equiv [\mathbf{v}(\mathbf{x} + \mathbf{r}) - \mathbf{v}(\mathbf{x})] \cdot [\mathbf{r}/r]$, which scales as $S_p(r) \sim r^{\zeta_p}$, for $\eta_d \ll r \ll L$, where η_d is the dissipation length scale below which viscous dissipation is significant, L is the large length scale at which energy is injected into the fluid, and the multiscaling exponents ζ_p , which are nonlinear, monotone increasing functions of p , characterize the intermit-

tency [1]; simple scaling is obtained if ζ_p depends linearly on p as in the phenomenological approach (K41) of Kolmogorov [17].

The determination of ζ_p is a challenging task [5, 6, 9], which is especially more difficult for time-dependent structure functions [18, 19] or MHD turbulence [12–16]. Therefore, we explore other signatures of intermittency. For three-dimensional (3D) fluid turbulence Refs. [20–22] have introduced a new way of analyzing direct numerical simulations (DNSs) to obtain fresh insights into suitably scaled (see below), order- m moments D_m of the vorticity $\omega = \nabla \times \mathbf{u}$. These studies show the following: (a) on theoretical grounds, three regimes, I, II, and III, are possible, with the D_m ordered in different ways (Fig. 1, Ref. [22]); but (b) *only regime I is observed in a wide variety of DNSs* [20–22]. Regime I has sufficiently depleted nonlinearity so that a global attractor exists, *if the solutions remain in region I*, as they do in all the DNSs examined so far from

this point of view.

We develop the analog of the above theoretical framework for the case of 3D MHD turbulence; then we examine the behaviors of D_m^\pm , the 3D MHD counterparts of D_m , in a variety of DNSs, which we have carried out independently in different groups, to obtain new insights into the depletion of nonlinearity here. We find that 3D MHD turbulence is like its fluid-turbulence counterpart inasmuch as all solutions remain in *only one regime, with depleted nonlinearity, in a large variety of DNSs*. We examine the implications of our results for the exponents q^\pm that characterize the power-law dependences of the energy spectra $\mathcal{E}^\pm(k)$ on the wave number k , in the inertial range of scales, ($2\pi/k$ much less than the energy-injection length scale and much greater than the length scale at which viscous and diffusive losses become significant).

The velocity \mathbf{u} and magnetic field \mathbf{b} can be combined into the Elsässer variables $\mathbf{z}^\pm = \mathbf{u} \pm \mathbf{b}$; with $\nu_\pm = [\nu \pm \eta]/2$, $\mathbf{f}^\pm = \mathbf{f}_u \pm \mathbf{f}_b$, the incompressible 3D MHD equations are

$$\partial_t \mathbf{z}^\pm + \mathbf{z}^\mp \cdot \nabla \mathbf{z}^\pm = -\nabla \mathcal{P} + \nu_+ \nabla^2 \mathbf{z}^\pm + \nu_- \nabla^2 \mathbf{z}^\mp + \mathbf{f}^\pm, \quad (1)$$

where $\nabla \cdot \mathbf{z}^\pm = 0$, \mathcal{P} is the total pressure, $\mathbf{j} = \nabla \times \mathbf{b}$ is the current density, and ν and η are, respectively, the kinematic viscosity and the magnetic diffusivity, whose ratio yields the magnetic Prandtl number $P_M = \nu/\eta$; and \mathbf{f}^\pm are the forcing terms, which are absent in decaying MHD turbulence. The Taylor-microscale Reynolds number $R_\Lambda = u_{rms} \sqrt{\langle \mathbf{u}^2 \rangle + \langle \mathbf{b}^2 \rangle} / (\nu \sqrt{\langle \boldsymbol{\omega}^2 \rangle + \langle \mathbf{j}^2 \rangle})$, with u_{rms} the root-mean-square velocity. Our DNSs of the 3D MHD equations use a periodic cubic box and a pseudospectral method [12–16] with large-scale initial conditions, and in some cases, forcing (Table I [23]).

For ideal 3D MHD (i.e., $\nu_\pm = 0$, $\mathbf{f}^\pm = 0$) the invariants are the energies $E_\pm = \frac{1}{2} \langle \mathbf{z}_\pm \cdot \mathbf{z}_\pm \rangle = E_T \pm H_C$ and the magnetic helicity $H_M = \langle \mathbf{A} \cdot \mathbf{b} \rangle$, where the vector potential \mathbf{A} yields $\mathbf{b} = \nabla \times \mathbf{A}$, $E_T = \frac{1}{2} \langle \mathbf{u} \cdot \mathbf{u} + \mathbf{b} \cdot \mathbf{b} \rangle = E_u + E_b$, and $H_C = \langle \mathbf{u} \cdot \mathbf{b} \rangle$. We define $\sigma_C = \cos(\mathbf{u}, \mathbf{b})$ and $\sigma_m = \cos(\mathbf{A}, \mathbf{b})$, the relative rates of cross and magnetic helicity, with $|\sigma_{c,m}| \leq 1$; they represent the degree to which the fields are aligned and they are measures, global or point-wise, of the strength of nonlinearities in MHD.

We obtain the evolution of the vorticity and the current, and thus of $\boldsymbol{\omega}^\pm = \boldsymbol{\omega} \pm \mathbf{j}$, by using standard vector identities [23]; for $P_M = 1$ we have

$$\begin{aligned} (\partial_t + \mathbf{z}^\mp \cdot \nabla) \boldsymbol{\omega}^\pm - \boldsymbol{\omega}^\mp \cdot \nabla \mathbf{z}^\pm - \nu \Delta \boldsymbol{\omega}^\pm - \nabla \times \mathbf{f}^\pm \\ = \boldsymbol{\omega}^\mp \times \boldsymbol{\omega}^\pm + \sum_{i=1}^3 \partial_i \mathbf{z}^\pm \times \partial_i \mathbf{z}^\mp. \end{aligned} \quad (2)$$

The two terms on the right-hand side stem from stem from the equation for the current; the labels $i = 1, 2$, and 3 refer respectively to x, y , and z [23].

The exact constraints because of conservation laws involve mixed (\mathbf{u}, \mathbf{b}) correlators [24, 25]. Dimensional analysis gives $\zeta_p^{IK} = p/4$, if we use the model of Iroshnikov and Kraichnan (IK) [26, 27] and assume $\sigma_C = 0$, or $\zeta_p^{K41} = p/3$, if we use K41 [16, 17]; and $\mathcal{E}^\pm(k) \sim k^{-3/2}$ (IK) or $\mathcal{E}^\pm(k) \sim k^{-5/3}$ (K41). Some models [28, 29] and DNS results [16, 30, 31] indicate that the departure from linear scaling, be it of the IK or K41 forms, is stronger in 3D MHD turbulence than it is in 3D Navier-Stokes (NS) turbulence, which suggests a depletion of nonlinearity by virtue of the tendency of alignment or anti-alignment of \mathbf{u} and \mathbf{b} .

We now describe our generalization of the analysis of Refs. [20–22], for the 3D NS equation, to the case of the 3D MHD equation [23]. We define the order- m scaled moments of $\boldsymbol{\omega}^\pm$:

$$\Omega_m^\pm(t) = \left(L^{-3} \int_V |\boldsymbol{\omega}^\pm|^{2m} dV \right)^{1/2m}; \quad (3)$$

$$D_m^\pm = (\varpi_0^{-1} \Omega_m^\pm)^{\alpha_m}, \quad \alpha_m = \frac{2m}{4m-3}; \quad (4)$$

here $\varpi_0 = \nu L^{-2}$ is the box-size frequency and the total volume $V = L^3$. A Hölder inequality implies that $\Omega_{m+1}^\pm(t) \geq \Omega_m^\pm(t) \geq \dots \geq \Omega_1^\pm(t)$; however, the D_m^\pm moments can scale with order m in different ways because α_m is a decreasing function of m . The choice of D_m , and the value of α_m [20], for the 3D NS equation, follow from the invariance of this equation under the transformations $\mathbf{x}' = a\mathbf{x}$, $t' = a^2 t$, $\mathbf{u}' = a^{-1}\mathbf{u}$, $\mathcal{P}' = a^{-2}\mathcal{P}$. For 3D MHD we must add $\mathbf{b}' = a^{-1}\mathbf{b}$; and we can then show that $\Omega_m^{\pm'} = [a^{-1/\alpha_m}] \Omega_m^\pm$ and define the coefficients $A_m^\pm(t) \equiv \ln D_m^\pm(t) / \ln D_1^\pm(t)$.

We follow [21, 22] and introduce the Ansätze [32]

$$D_1^{\pm \frac{\sigma}{2}} \leq D_m^\pm \leq D_1^{\pm A_{m,\lambda}^\pm}, \quad A_{m,\lambda}^\pm = \frac{m\lambda^\pm + 1 - \lambda^\pm}{4m-3}, \quad (5)$$

where $A_{m,\lambda}^\pm$ is the maximum over time of $A_m^\pm(t)$ and $1 \leq \lambda_\pm \leq 4$, which implies that the nonlinearity is depleted here (cf. Eq.(1.4) and compare Eq.(3.7) and Eq.(3.12) in Ref.[22]). The lower bounds on λ^\pm follow from the Hölder inequality $\Omega_m^\pm \geq \Omega_1^\pm$; the upper bounds are treated as in the NS case [22].

We have more variables in the 3D-MHD case than in the 3D NS equation, so we introduce $X_1 \equiv D_1^+ + D_1^-$ and show [23]

$$\frac{\dot{X}_1^\pm}{2\varpi_0} \leq -\frac{X_1^2}{2E_0} + c_{6,m}X_1^{1+\frac{1}{2}\lambda^\pm - \frac{(\lambda^\pm - \lambda^\mp)}{4m}} + GrX_1^{1/2}, \quad (6)$$

where E_0 is a bounded and dimensionless measure of the energy, Gr the Grashof number, a dimensionless measure of the forcing term, and $c_{6,m}$ a constant. Hence, X_1 remains bounded if the negative term on the right-hand side of (6) dominates, which occurs if

$$1 + \frac{1}{2}\lambda^\pm - (\lambda^\pm - \lambda^\mp)/4m < 2, \quad (7)$$

or equivalently $\lambda^\pm < 2 + \epsilon_m^\pm$, where $\epsilon_m^\pm = (\lambda^\pm - \lambda^\mp)/2m$ is a small number [36]. Therefore, the *natural*, 3D-MHD analogs of Fig. 1 in Ref. [22] are the schematic plots of D_m^\pm versus D_1^+ and D_m^- versus D_1^- in Fig. 1, which show three regimes: For regular solutions, we must have $1 \leq \lambda^\pm \leq 2$ (regime I); when $2 \leq \lambda^\pm \leq 4$ (regime II), there is depletion, but not enough to control solutions; and, finally, at $\lambda_\pm = 4$ (regime III) we have $D_m^\pm \propto D_1^\pm$.

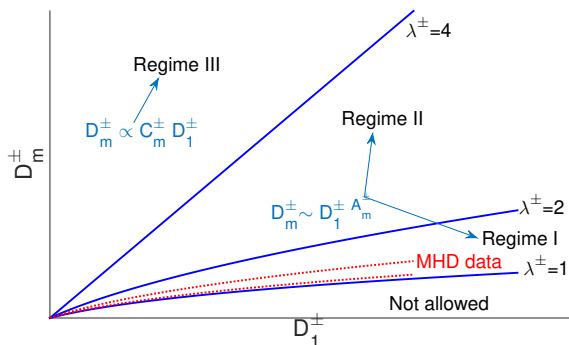


FIG. 1: (Color online) Schematic plots of D_m^+ versus D_1^+ and D_m^- versus D_1^- showing the three regimes I, II, and III for 3D MHD. Regularity can be proven if both D_1^+ and D_1^- lie in regimes I or III.

Our DNS data [23] indicate that regime I ($1 \leq \lambda^\pm \leq 2$) is obtained in 3D MHD for all the solu-

tions we study. In Fig. 2 we give representative results from four of our DNSs [23]. In the first column of Fig. 2, we give log-log (base 10) plots of the energy spectra $E(k)$ versus k ; the second column has plots of $A_m^+(t)$ versus t , from which we determine $A_{m,\lambda}^+$ (plots for $A_m^-(t)$ versus t are similar), which follow from $D_m^+(t)$.

Numerical trajectories do not follow exactly the schematic, concave curves of Figs. 1 (a) and (b), so we determine λ^\pm as follows (cf. Ref. [22] for the 3D-NS equation). We define λ_m^\pm to be those values that we compute from Eq. (5) for $A_{m,\lambda}^\pm$. In the third column of Fig. 2, we give plots of λ_m^\pm versus m , in the range $2 \leq m \leq 9$, for which we obtain good-quality numerical data. From these plots we obtain λ^\pm from the minimum over m of λ_m^\pm . In general, $1 \leq \lambda_\pm \leq 4$; however, in all our DNSs, $1 \leq \lambda_\pm \leq 2$, i.e., our solutions lie in regime I.

To examine the implications of our results for energy spectra, we define the dimensionless, time-averaged, inverse length scale $\kappa_{2,0} = \left[\frac{\|\nabla \omega^\pm\|_2}{\|z^\pm\|_2} \right]^{1/2}$ and obtain [23]

$$\langle L\kappa_{2,0}^\pm \rangle_T \leq c Re^{\frac{\lambda^\pm+1}{4} + \frac{\lambda^\mp}{8}}, \quad (8)$$

where $Re = L\sqrt{2E_{\text{tot}}}/\nu$ is the *global* Reynolds number and $\langle \rangle_T$ stands for temporal average. If we assume isotropy and make the power-law Ansatz

$$\mathcal{E}^\pm(k) = \begin{cases} A k^{-q^\pm}, & L^{-1} \leq k \leq k_c^\pm, \\ 0, & k > k_c^\pm, \end{cases} \quad (9)$$

we obtain

$$\langle L\kappa_{2,0}^\pm \rangle_T \sim (Lk_c^\pm)^{1 - \frac{q^\pm - 1}{4}} \sim Re^{\frac{5-q}{4(3-q)}}, \quad (10)$$

(see Eqs.(??-??) in [23]). We thus get

$$q^\pm \geq 3 - \frac{4}{2\lambda^\pm + \lambda^\mp} \geq \frac{5}{3}, \quad (11)$$

which excludes the IK exponent $3/2$, at least in the absence of intermittency. However, we have assumed full isotropy at all scales and the limit $Re \rightarrow \infty$ when comparing (8) and (10). Furthermore, (10) implicitly assumes $E_+ = E_-$. In the general [23], this relation is modified leading to a set of inequalities for the q^\pm that do not exclude IK.

In Fig. 3 we display plots of $\langle D_m^+ \rangle$ versus R_Λ , where the angular brackets now indicate the average over the statistically stationary turbulent

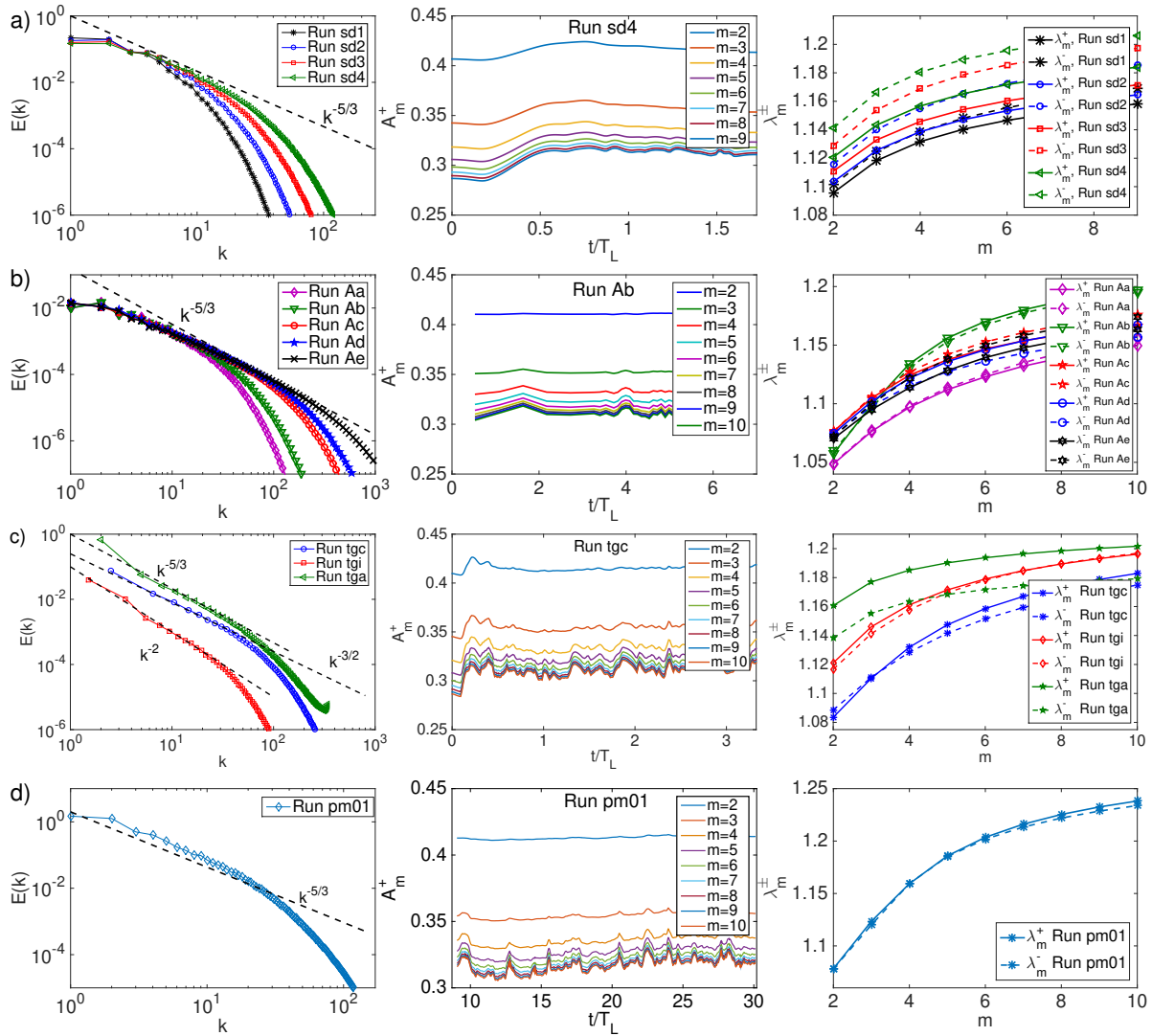


FIG. 2: (Color online) Representative results from our DNSs: total energy spectra (first column), temporal evolution of A_m^\pm (second column) and values of λ_m^\pm (third column). The rows correspond to different runs: a) decaying 3D MHD turbulence, b) forced, statistically steady 3D MHD turbulence, c) forced, statistically steady 3D MHD turbulence with imposed Taylor-Green symmetries and d) forced, statistically steady 3D MHD turbulence with $P_M = 0.1$. For parameters see Table 1 in [23]

state; we present data (pentagrams in Fig. 3) from the runs Aa-Ae (Table I in [23]). Circles indicate decaying-MHD data points (runs sd1-sd4); here we use the value of D_m^+ at the time at which the energy-dissipation rate ϵ reaches its first maximum [16]. The order- m moments of gradients, or *gradmoments*, of hydrodynamic fields have been used to investigate Nelkin scaling [33–35], i.e., the power-law dependence of the gradmoments on the Reynolds number Re in the case of fluid turbulence; the Nelkin-scaling exponents ξ_m can be related to the structure-function exponents ζ_m [33–

35]. Our vorticity moments are upper bounds for gradmoments of the Elsässer variables by virtue of the Riesz transform (see Eq. (1.11) in [23]). If these bounds are saturated, then the exponents, which we extract from the plots of Fig. 3, should be related to the Nelkin exponents for 3D MHD turbulence. We defer a detailed exposition of such scaling in 3D MHD to another study.

In liquid metals, as well as in the solar photosphere, P_M is very small. It can also be very large as, e.g., in the interstellar medium. Our mathematical analysis in [23] is not valid if $P_M \neq 1$ be-

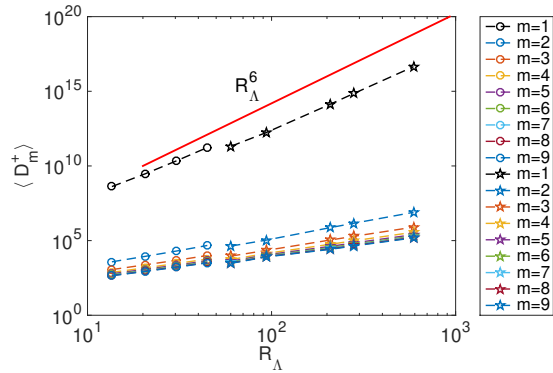


FIG. 3: (Color online) Plots versus R_Λ of $\langle D_m^+ \rangle$, for the runs Aa-Ae (pentagrams) and its decaying-MHD analog, for the runs sd1-sd4 (circles), where we use the value of D_m^+ at the time at which the energy dissipation rate ϵ reaches its first maximum [16]. See Table I in [23] for additional information about these runs.

cause ν_- can become negative for $P_M \leq 1$. However, our DNS results in Fig. 3 show that plots for $P_M = 0.1$ (bottom row) are similar to their counterparts for $P_M = 1$ (top three rows). Furthermore, we see from Table ?? (Supplemental Material [23]), at least for a fixed value of ν , that the values of λ_m^\pm are comparable to their $P_M = 1$ counterparts; these values of λ^\pm decrease marginally as we increase P_M .

Our work, which builds upon the studies of Refs. [20–22] for fluid turbulence, provides new insights into the depletion of nonlinearity in 3D MHD turbulence and its intermittency. In particular, we introduce the scaled moments D_m^\pm , and then obtain inequalities containing D_m^\pm and D_1^\pm ; these inequalities specify three possible regimes. We find that 3D MHD turbulence is like its fluid-turbulence counterpart insofar as all solutions, which we have investigated, remain in only one regime; this regime I (Fig. 1) displays depleted nonlinearity. Our results lead to the inequality (11) for the spectral exponents q^\pm , if we make the assumption of isotropy. We suggest that the Riesz transform can relate D_m^\pm and the order- m moments of gradients of the hydrodynamic fields; such moments can then be used, along with a suitable generalization of Nelkin scaling [33–35] for 3D MHD turbulence, to relate slopes of plots like those in Fig. 3 to the multiscaling exponents of Elsässer-field structure functions. We conclude that 3D MHD appears to have more nonlinear

depletion than does fluid turbulence, because the values of λ^\pm are lower than those for their fluid-turbulence counterparts; this can be attributed to Alfvén waves weakening the nonlinear eddies.

Acknowledgments: We thank H. Homann and R. Grauer for providing the data of runs Ad and Ae. Data from runs Ad and Ae of H. Homann and R. Grauer was produced on the IBM BlueGene/P computer JUGENE at the FZ Juelich that was available through the “XXL project of HBO28”. We also acknowledge U. Frisch and D. Vincenzi for useful discussions. The computations for runs sd1-sd4 were performed on Janus (CU Boulder). Runs Aa-Ac and tg were performed at Mésocentre SIGAMM hosted at the Observatoire de la Côte d’Azur and CICADA hosted by the University of Nice-Sophia. Computer time was also provided by GENCI on the IDRIS/CINES/TGCC clusters. JG and AP thank Fédération Doebelin for support. RP thanks the Department of Science and Technology (India) for support and SERC (IISc) for computational resources. AG is grateful for support through a grant from the European Research Council (ERC) under the European Community’s Seventh Framework Programme (FP7/2007-2013)/ERC Grant Agreement No. 297004. GS acknowledges support from the ERC Advanced Grant “NewTURB”, No. 339032. GK thanks the Indo-French Centre for Applied Mathematics (IFCAM) for supporting a visit during which parts of this paper were written. JS is supported by the National Science Foundation (NSF) Graduate Research Fellowship Program (GRFP) under Grant No. DGE 1144083.

-
- [1] U. Frisch, *Turbulence: The Legacy of A. N. Kolmogorov* (Cambridge University Press, Cambridge, 1995).
 - [2] R. Kerr, *J. Fluid Mech.* **153**, 31 (1985).
 - [3] C. Meneveau and K. R. Sreenivasan, *J. Fluid Mech.* **224**, 429 (1991).
 - [4] K. R. Sreenivasan and R. A. Antonia, *Ann. Rev. Fluids Mech.* **29**, 435 (1997).
 - [5] G. Boffetta, A. Mazzino, and A. Vulpiani, *J. Phys. A: Mathematical and Theoretical* **41**, 363001 (2008).
 - [6] A. Arneodo, R. Benzi, J. Berg, L. Biferale, E. Bodenschatz, A. Busse, E. Calzavarini, B. Castaing, M. Cencini, L. Chevillard, et al., *Phys. Rev. Lett.*

- 100**, 254504 (2008).
- [7] D. Donzis, P. Yeung, and K. Sreenivasan, *Phys. Fluids* **20**, 045108 (2008).
- [8] T. Ishihara, T. Gotoh, and Y. Kaneda, *Annu. Rev. Fluid Mech.* **41**, 16 (2009).
- [9] R. Pandit, P. Perlekar, and S. S. Ray, *Pramana, Journal of Physics* **73**, 157 (2009).
- [10] S. Bramwell, P. Holdsworth, and J. Pinton, *Nature* **396**, 552 (1998).
- [11] D. Sornette, Springer-Verlag Berlin Heidelberg (2006).
- [12] D. Biskamp and W.-C. Mueller, *Phys. Plasmas* **7**, 4889 (2000).
- [13] W.-C. Mueller and D. Biskamp, *Phys. Rev. Lett.* **84**, 475 (2000).
- [14] P. Mininni and A. Pouquet, *Phys. Rev. Lett.* **99**, 254502 (2007).
- [15] P. Mininni and A. Pouquet, *Phys. Rev. E* **80**, 025401 (2009).
- [16] G. Sahoo, P. Perlekar, and R. Pandit, *New J. Physics* **13**, 013036 (2011).
- [17] A. N. Kolmogorov, *Dokl. Akad. Nauk SSSR* **32**, 16 (1941).
- [18] D. Mitra and R. Pandit, *Phys. Rev. Lett.* **93**, 024501 (2004).
- [19] S. S. Ray, D. Mitra, and R. Pandit, *New J. Phys.* **10**, 033003 (2008).
- [20] J. Gibbon, *J. Math. Phys.* **53**, 115608 (2012).
- [21] D. Donzis, J. Gibbon, A. Gupta, R. Kerr, R. Pandit, and D. Vincenzi, *J. Fluid Mech.* **732**, 316 (2013).
- [22] J. Gibbon, D. Donzis, A. Gupta, R. Kerr, R. Pandit, and D. Vincenzi, *Nonlinearity* **27**, 2605 (2014).
- [23] Supplementary material (2015).
- [24] H. Politano, T. Gomez, and A. Pouquet, *Phys. Rev. E* **68**, 026315 (2003).
- [25] A. Basu, A. Naji, and R. Pandit, *Phys. Rev. E* **89**, 012117 (2014).
- [26] P. S. Iroshnikov, *Sov. Astron.* **7**, 566 (1963).
- [27] R. H. Kraichnan, *Phys. Fluids* **8**, 1385 (1965).
- [28] R. Grauer, J. Krug, and C. Mariani, *Phys. Lett. A* **195**, 335 (1994).
- [29] H. Politano and A. Pouquet, *Phys. Rev. E* **52**, 636 (1995).
- [30] H. Politano, V. Carbone, and A. Pouquet, *Europhys. Lett.* **43**, 516 (1998).
- [31] W. Müller, D. Biskamp, and R. Grappin, *Phys. Rev. E* **67**, 066302 (2003).
- [32] J. D. Gibbon, ArXiv:1506.03060v2 (2015).
- [33] M. Nelkin, *Phys. Rev. A* **42**, 7226 (1990).
- [34] J. Schumacher, K. R. Sreenivasan, and V. Yakhot, *New J. Phys.* **9**, 89 (2007).
- [35] S. Chakraborty, U. Frisch, W. Pauls, and S. S. Ray, *Phys. Rev. A* **42**, 7226 (1990).
- [36] Standard analysis leads to a term $\propto X_1^3$ in Eq.(6) (see Ref. [22] for the NS case), which does not lead to a control over the solutions at large times.